

N88-14890516-16

116679
228

RAMAN SPECTRA OF ADSORBED LAYERS ON SPACE SHUTTLE AND
AOTV THERMAL PROTECTION SYSTEM SURFACE

N4368087

Final Report

NASA/ASEE Summer Faculty Fellowship Program--1987

Johnson Space Center

Prepared by:	Ronald J. Willey, Ph.D.
Academic Rank	Assistant Professor
University & Department	Northeastern University Department of Chem. Eng. Boston, MA 02115
NASA/JSC	
Directorate:	Engineering
Division:	Structures & Mechanics
Branch:	Thermal
JSC Colleagues:	John E. Grimaud Carl D. Scott, Ph.D.
Date:	3 September 1987
Contact Number:	NGT 44-001-800

ABSTRACT

Surfaces of interest to space vehicle heat shield design were struck by a 2 W argon ion laser line while subjected to supersonic arc jet flow conditions. Emission spectra were taken at 90° to the angle of laser incidence on the test object. Results showed possible weak Raman shifts which could not be directly tied to any particular parameter such as surface temperature (range 900 to 1,500 K), or gas compositions (air, O_2/N_2 mixture, N_2 , and argon).

The investigation must be considered exploratory in terms of findings. Many undesirable effects were found and corrected as the project progressed. For instance, initial spectra settings lead to ghosts (stray light within the spectrometer) which were eliminated by closing the intermediate of filter slit of the Spex from 8 mm to 3 mm. Further, under certain conditions, plasma lines from the laser were observed. Several materials were also investigated at room temperature for Raman shifts. Results showed Raman shifts for RCC and TEOS coated materials. HRSI materials showed only weak Raman shifts, however, substantial efforts were made in studying these materials. Baseline materials showed the technique to be sound (Raman spectra of quartz and a silicone grease were checked). The original goal was to find a Raman shift for the HRSI RCG coated material and tie the amplitude of this peak to Arc jet conditions. Weak Raman shifts may be present, however, time limitations preventive confirmation.

BACKGROUND

The Raman effect involves inelastic collisions of a beam of light (photons) which strike a surface or gas molecule. The photons, which strikes the surface, can give up of a portion of their energy to the surface molecules (in a quantum amount which is characteristic of the surface molecules). These photons then exit the surface at lower energy and their frequency is "shifted" to a lower wavenumber. The Raman effect or Raman shift was first predicted by Adolf Smekal in 1923. Sir Chandrasekhara Venkata Raman experimentally demonstrated the shift around 1927. The effect is quite weak with an intensity of about 1/100,000 of the incident beam (most collisions are elastic).

The application of Raman spectroscopy to surface science has expanded tremendously in the past 5 years. Improvements in data acquisition by microcomputers and in high speed A/D converters have opened up the ability to record low power light sources such as those generated by a Raman shift. Surface Raman spectroscopic techniques have been applied to many materials primarily of catalytic nature. Recent works include the adsorption of methane onto silica (Morrow, 1980) and the characterization of nickel oxide states on alumina catalysts (Wachs et al., 1986).

Raman spectroscopy ties into the Johnson Space Center Atmospheric Reentry Materials and Structures Evaluation Facility (Arc Jet) because of recent acquisition of a 5 W argon ion laser and a Spex Model 1877 triple spectrometer. With this equipment, surface Raman is a possible technique to use to characterize and better understand reusable heatshield materials under conditions which simulate reentry.

The design of reusable heatshield materials require 3 major design criteria: stability, ability to shed radiation to the surroundings, and be non-catalytic. It is the third criteria, a non-catalytic surface, where surface Raman may provide fundamental information. The current workhorse heatshield material is high temperature reusable surface insulation (HRSI) which is composed of alumina and silica fibers coated with a reaction cured borosilicate glass (RCG). The RCG coating is an excellent radiator and is pretty much non-catalytic, however, a small amount of atom recombination can occur (Kolodziej and Stewart, 1987). Therefore, heat shield design must take into account this factor. The problem however is that fundamental mechanisms have been lacking.

Recently, Seward, 1985, has proposed a recombination mechanism which predicts an interesting and critical result: a peak in the recombination rate with temperature. Seward's model is based on the following mechanism:



and his resultant model:

$$\text{recombination coefficient} = \frac{2 P S_o N \exp (-E/kT)}{S_o N + P N \exp (-E/kT) + \Delta}$$

where:

S_o is the sticking coefficient

N is the atomic flux to the surface

P is the steric factor

k is the Boltzmann constant

T is the temperature

E is the activation energy for the forward reaction 2

Δ is thermal desorption rate which is a function of temperature = $C_a (kT/h) \exp (-D/k T)$

where:

C_a is the number of adsorption sites per unit area

D is the thermal desorption energy

Equation two predicts a transition from zero order to first order for the recombination coefficient in oxygen partial pressure when the thermal desorption begins to be important (the reverse Reaction 1). It should be noted that N depends on the first order of oxygen concentration. Further, because of the predicted Arrhenius behavior for thermal desorption, the predicted recombination coefficient takes a nose dives to practically zero above its peak temperature. Experimentally, Kolodziej and Stewart, 1987, have reported recombination coefficients dropping above a certain temperature. Thus an initial objective of this work was to see if a Raman shift could be found which was associated with Si-O bonds on HRSI materials, and further, how did the Si-O bond alter under various arc jet conditions such as current and gas compositions.

EXPERIMENTAL

EQUIPMENT DESCRIPTION

Figure 1 represents a schematic diagram of the equipment used in this work. At the heart of the work was Model Spex 1877 0.6 m triple spectrometer. Light from the arc tunnel was focused through a 38 OD 75 fl lens through a 400 nm low wavelength filter past a mirror through another lens (a 76 OD 250 fl) into the entrance slit of the spectrometer. A 150 groove/mm filter grating filtered light before it reached the main spectrometer entrance slit. For this work the main spectrometer grating was set at 600 grooves/mm (two other settings are possible). Light diffracted by the

To Optical Multichannel Analyzer

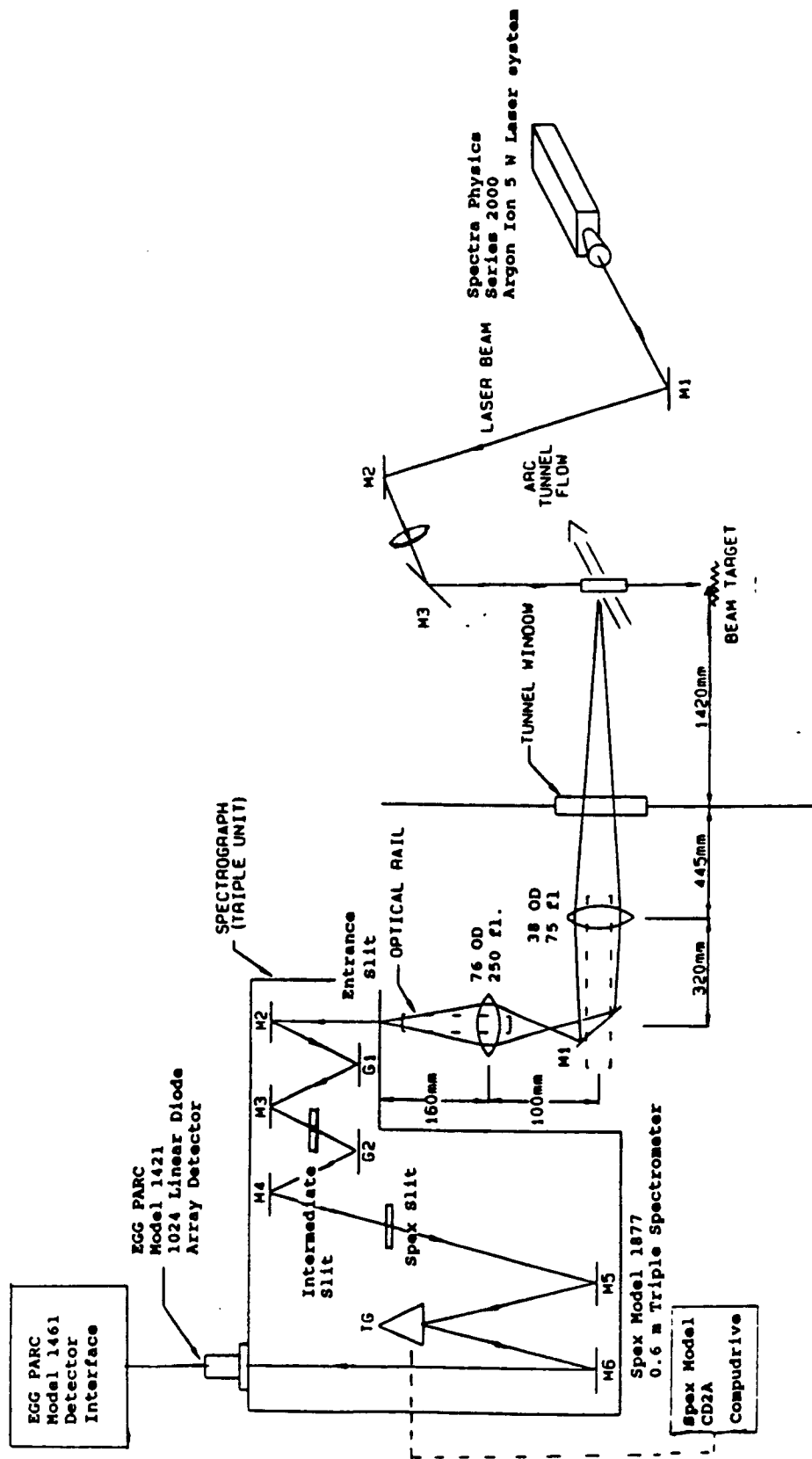


Figure 1. Apparatus Diagram.

spectrometer was collected by a EG&G PARC Model 1421 diode array which consisted of 1024 diodes sensitive in the UV and visible range. The diode array was interfaced to an optical multichannel analyzer (OMA) via a EG&G PARC Model 1461 detector interface. The OMA allowed the collection of spectroscopic data onto hard or soft disk for latter analysis such as plotting by a HP 7440 plotter or intensity analysis by a Epson FX 85 printer. The OMA also controlled the spectrograph wavelength setting (via a BASIC program written by Dr. Fred Wierum), scan times, and number of scans collected. Minimum scan time was 16.63 milliseconds across a wavelength range of 70 nm. Up to about 30,000 scans per collection period were possible.

Raman scattering was made possible by the use of a Spectra Physics Series 2000 argon ion laser system. The laser had two major excitation lines at 514.536 nm and 488.0 nm. The beam for the laser was focused into the centerline of the arcjet tunnel by 3 mirrors and one lens with a focal point of 1.5 m.

OPERATION

An example experimental start-up and operation procedure will be presented. The first step involved turning on the Spex spectrograph and entering the wave length into Spex CD2A compudrive to insure that the grating position matched the compudrive position. Then two configuration changes were made on the compudrive. Next, the N₂ purge gas flow was checked and set at 130 units on the rotameter. Then, the Model 1461 A/D converter was turned on. Then, one proceeded to the control room to turn on the printer, the plotter, and then the OMA system. The software was booted up and the system now ready. Full detailed directions have been written by Dr. Wierum and should be followed.

The laser control box was turned on lifting the main electrical switch up. Water flow was turned on and the water flow adjusted to 3 gallons per minute. After a 10 minute warm up the magnetic current was set at 9 amps and the current was set to about 38 amps. Under these conditions the laser would emit a line at 514.536 nm of about 2 watts in power. The laser line was then focused into the arc jet by adjusting each mirror in the optical train working from the laser source. Final focusing was done by adjusting the laser line intersection point with the optical path of the spectrometer and hitting the desired target (a space shuttle tile). Special argon laser line protective glasses were worn during the laser operation and mirror adjustment procedure.

For runs involving the arc jet, gas flow rates were set at 0.045 kg/sec (0.1 lb/sec). Currents ranged from 400 to 1200 amps depending on what conditions were being evaluated. The heated gases flowed through a 2.25 inch diameter throat and exited through a 15 inch diameter nozzle set at a 15 degree half angle. Under the condition studied the exit velocity was about 4,000 m/s at a Mach number of 7.0. Test articles evaluated in the arc jet flow were a 4 1/2 " X 5 " wedge inserted into a copper holder and a 2" radius HRSI RCG coated hemisphere model. Run numbers for this work were 2-563-SD to SD-574-SD. Further run details may be obtained from arc jet personnel. Table 1 is a brief summary of arc jet conditions run.

The laser used was a Argon Ion laser with a tunable excitation lines of 488 or 514.5 nm. Lower powered laser lines are also available at 457.9, 465.8, 472.7, 476.5, 496.5 and 501.7 nm.

TABLE 1. SUMMARY OF ARC JET CONDITIONS EVALUATED FOR RAMAN SHIFTS ON HRSI

Test Articles:

HRSI Wedge 4 1/2" X 5" inserted into a copper leading edge holder

HRSI Hemisphere of 2" in radius

Arc Jet Conditions:							Typical Surface Temperatures, Kelvin	
Mass Flow Rate kg/sec	Gas Composition		Mass %	Current Amps	Power MW	Enthalpy MJ/kg	Wedge	Hemisphere
	O ₂	N ₂						
AIR								
0.0454	24.00	76.00	0.00	400.00	1.03	11.88		1429.44
0.0454	24.00	76.00	0.00	500.00	1.24	15.24	962.78	1477.78
0.0454	24.00	76.00	0.00	700.00	1.61	18.00	1002.22	
0.0454	24.00	76.00	0.00	900.00	1.98	18.62	1042.78	
0.0454	24.00	76.00	0.00	1200.00	2.52	19.03	1068.89	
Mixtures								
0.0454	6.00	94.00	0.00	500.00	1.31	17.23	932.78	
0.0454	10.00	90.00	0.00	500.00	1.30	17.53	914.44	
0.0454	21.60	68.40	10.00	500.00	1.26	11.50	941.67	
Nitrogen								
0.0454	0.00	100.00	0.00	400.00	1.08	11.42		1291.11
0.0454	0.00	100.00	0.00	500.00	1.32	15.91	956.11	1446.67
0.0454	0.00	100.00	0.00	900.00	2.12	22.46	1011.67	
0.0454	0.00	100.00	0.00	1200.00	2.52	19.03	1068.89	
Argon								
0.0454	0.00	0.00	100.00	500.00	0.12		797.78	553.89

Alignment was accomplished by focusing a helium-neon laser through the Spex optical path onto the test article located in the test position. This was made easy by using the Spex's side exit for the helium-neon laser and setting the Spex at the laser's wavelength (632.8 nm). Once the "red dot" was located, the "green" line from the argon laser was focused through its mirror system down into the test chamber. Final alignment required that the "green dot" strike the "red dot" on the test article. This approach assured that the Spex would be looking at a region excited by the argon laser line.

After alignment, the neon laser was turned off and the side entrance closed. The side exit mirror was then changed to straight pass. The spectrometer was then reset to a centering wavelength of 560 nm (280 on the compudrive and 140 on the filter setting). The entrance slit was adjusted to 1.0 mm, the intermediate slit to 2.8 mm and the Spex slit to 600 microns. For these settings with a 514.6 nm laser excitation line, the wavelength range is 240 to 2500 cm^{-1} . For a wavenumber range of 2,200 cm^{-1} to 4,000 cm^{-1} the Spex was reset to a center wavelength of 616 nm (308 on the compudrive and 154 on the filter). The intermediate slit was reset to 3.2 mm.

Several operating conditions for the OMA were examined. Scan exposure times of 16.63 ms to 12,000 ms were used. Longer exposure times eliminated noise, however, one must watch for overloading the photo diode array (>16,000 counts per scan). Multiple collections are also possible. A range of 1 to 30,000 scans could be collected. The best operating condition found was an exposure at 100 ms for 100 or 1,000 scans.

FINDINGS

CALIBRATION

Scale calibration was accomplished by calculating wavenumbers for neon lamp lines at various Spex settings. The formula used was:

$$\text{Shift in } \text{m}^{-1} = (1/\lambda \text{ m}^{-1} \text{ excitation}) - (1/\lambda \text{ m}^{-1} \text{ neon})$$

$$\text{cm}^{-1} = 100 \text{ m}^{-1}$$

Because of the non linear nature of wavenumber to wavelength conversion, a cubic fit available on the OMA system was used. The summary of calibrations is presented in Table 2.

PRELIMINARY FINDINGS

After 2 months of preparation, the laser was turned on and the first set of Raman spectra were collected under arc jet conditions. A review of results showed narrow peaks of very high counts (2×10^6 at 16.63 seconds total exposure time). The top line in Figure 2 shows the narrow peaks observed. These peaks disappeared when the intermediate filter slit was closed from 8 mm to 7 mm (indicating stray light inside the Spex). Because of stray light, the Spex intermediate slit was closed down to 2.8 to 3.2 mm so that only the 70 nm required to fill the photo diode array would pass into the main spectrometer. A disadvantage to centering the filter to the Spex setting is

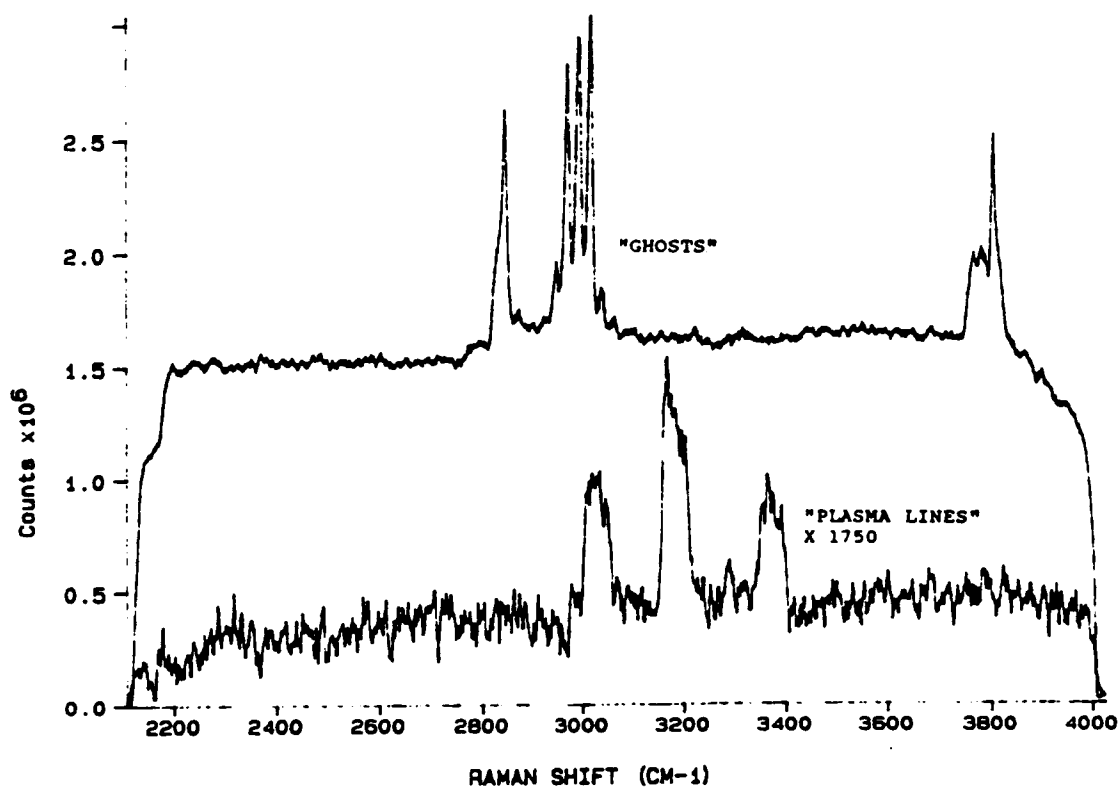


Figure 2. Ghosts and Plasma.

that it removes the ability to change wavelength remotely. Any grating change thus requires an arc off during a run.

Shown in the bottom half of Figure 2 is another anomaly discovered in the very weak spectrums - plasma lines. Plasma lines are atomic lines emitted from the laser whether it is lasing or not. These lines can be eliminated by a Model 1460 tunable excitation filter available from Spex Industries of Edison New Jersey. Time prevented the employment of a filter, however, it is recommended that one be purchased and put into use. To eliminate the influence of plasma lines in Raman spectra, background was taken in which the laser was left on however it was adjusted slightly off line so that it did not lase. Spectrum shown in the figures discussed below are for a background which includes the plasma radiation. Background spectra are referred to as plasma background.

TABLE 2. WAVENUMBER CALIBRATION DATA (Units cm^{-1})

Laser Excitation Line = 514.5 nm

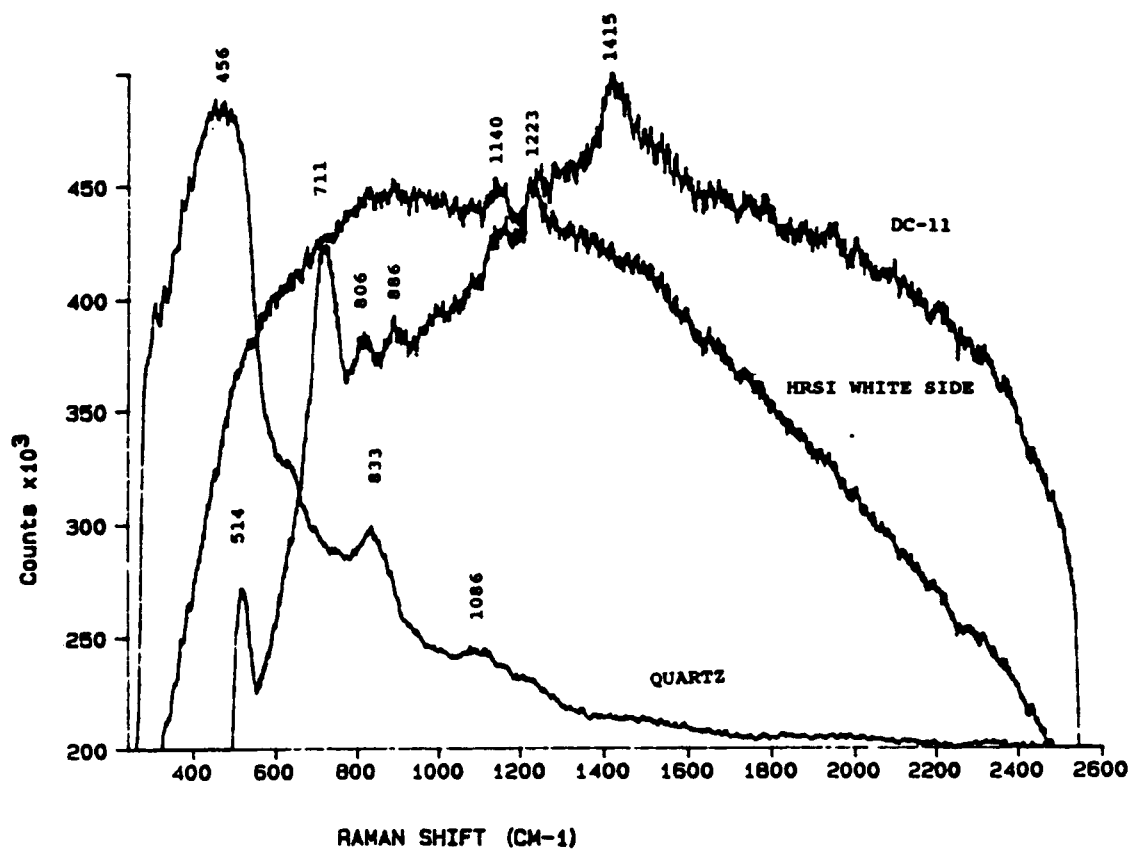
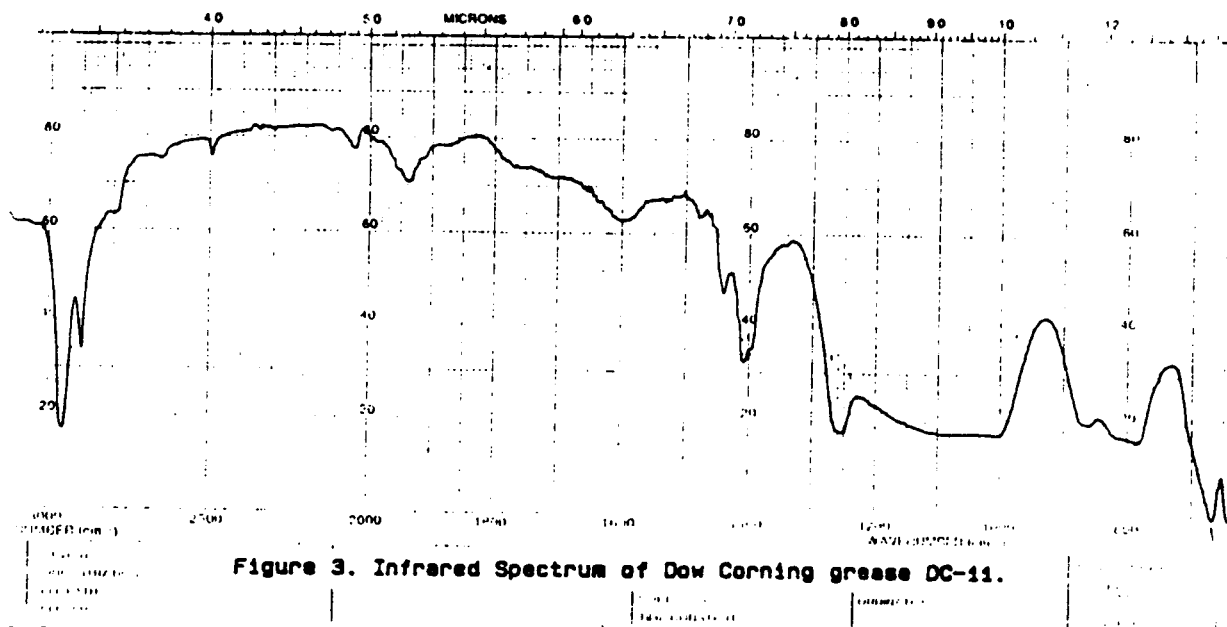
OMA File # on Drive 1	Centering Wavelength nm	A0	A1	A2 ($\times 10^4$)	A3 ($\times 10^7$)
636	560	237.035	2.76972	-8.062	3.206
637	616	2106.73	2.17466	-4.304	1.349
639	672	3642.32	1.75655	-1.875	9.316E-3

Laser Excitation Line = 488.0 nm

638	527	98.7479	2.91402	-4.557	0.7710
671	560	1314.23	2.65549	-6.100	2.205

MATERIAL SURVEY

Further investigation indicated the technique had to be checked. Dow Corning Silicon Grease, DC-11, was used for this check. DC-11's infrared spectrum, completed by Mr. Dwayne Caston of Lockheed, is shown in Figure 3. Peaks are seen at wavenumbers in cm^{-1} of 670 (s), 800 (b), 870 (w), 1100 (b), 1255 (m), 1410 (s), 1440 (w), 1600 (w), 1940 (w), 2020 (w), 2500 (w), 2900 (s) and 2950 (s). The small letters after the number have the following meaning: (s) for a strong peak, (m) for a moderate peak, (w) for a weak peak, and (b) for a broad peak. A Raman spectrum in the same wave number range on DC-11 is shown in Figures 4 & 5 (Raman spectrums for other materials are also shown in these figures). Peaks are seen in the Raman spectrum at wavenumbers of 514(s) (this is below the infrared results), 711 (s), 806 (w), 886 (w), 1123 (w), 1234 (w), 1415 (m), 2916(s), 2979 (s) cm^{-1} . This is an excellent match, however, relative



intensities are different. Further checks for Raman shifts at other laser excitation lines (488.0, 496.5, and 501.7) were made. In all cases, the peaks were found within 30 wavenumbers of those given above.

Other materials investigated for Raman shifts at room temperature are listed in Table 3. The Raman spectra for these various materials tested are shown in Figures 4, 5, & 6. All of these materials showed at least one good Raman shift or "peak" with the exception of HRSI RCG coated material. Wavenumbers of the peaks are also listed in Table 3. Full identification could not be made because of time limitations.

EMISSION AND RAMAN SPECTRA UNDER ARC JET CONDITIONS

Several experiments were conducted under arc jet conditions. Table 1, presented above, lists the conditions investigated.

Figure 7 shows the emission spectra for laser on and plasma background conditions for a hemisphere inserted into an arc jet flow of 0.0454 kg/sec of air at 400 and 500 amps. The stagnation point of the hemisphere was located 23.2 cm from the exit plane of the nozzle. The spectrometer focal point was 1.5 cm behind the stagnation point. The results showed several emission peaks. The eleven lines located between 528 to 541.1 nm are primarily related to nitrogen atoms with the 533 peak related to oxygen atoms. The broad band in the 576 nm and 583.6 nm are related to N_2 1st positive system $\Delta v = 4$. The broad peaks at 557.6 and 562.2 nm are currently not identified. More details about species identification for arc jet flow can be found in Willey, 1987.

Another example of emission spectra at a different location on the hemisphere is shown in Figure 8. The location is in a cooler region of 3.5 cm back of the stagnation point. The emission spectra is dampen somewhat. One trend that is observed is that the influence of the laser on the emission spectra is enhanced as temperature is lowered.

Figure 9 shows the difference or Raman spectra for the four conditions investigated above. Unfortunately, peaks which appear can be related back to the emission spectra. For example, the peak seen at 400 to 800 cm^{-1} are related to the atomic lines identified in Figure 7. The peak seen at 1500 cm^{-1} for the 500 amps point 1 condition appears because the difference between the valley for the laser minus background is greater than the surrounding difference seen in the neighboring peaks. Spectrometer settings for all data presented were a Spex slit opening of 600 microns, an intermediate slit opening of 2.8 mm at the 560 nm centering wavelength and 3.2 mm at the 616 nm centering wavelength.

Three emission peaks are seen at the higher wavelength range of 578 to 648 nm shown in Figure 10. The first peak at 589.3 nm is probably sodium, the second peak at 601.4 is probably 1st positive nitrogen, and the third peak at 616 nm is probably due to oxygen atoms. A repeated run is suggested at a lower Spex slit opening of 20 nm of so to check for atomic lines and molecular bands in this region.

Figure 11 is the difference spectra between the laser on and plasma background. The two peaks seen are tied to the emission peaks seen at 589.3 nm and 616 nm. An interesting observation is that the 601.4 peak did not excite as much as the other two peaks. Maybe this is a difference related to atomic versus molecular species. Other

TABLE 3. RAMAN SHIFTS OBSERVED FOR VARIOUS RAW MATERIALS AT ROOM TEMPERATURE

Material	Raman Shifts Observed (cm ⁻¹)	Possible Species
High Temperature Reusable Surface Insulation (HRSI)		
Reaction Cured Glass Coating (RCG)	2914 (vw)	
97% Borosilicate glass (5% B ₂ O ₃ ,	2932 (vw)	
95% SiO ₂) & 3% Silicon Tetraboride	3256 (vw)	
	3497 (vw)	
White Silica/Alumina Fibers	1133 (w)	Si-O-Si
	1234 (m)	Si-O-Si
	2462 (w)	
	2629 (vw)	
	2838 (m)	
	2905 (m)	
Reinforced Carbon Carbon (RCC)		
Silicon-Carbide Coated Side	583 (w)	Si-O-Si
	630 (w)	"
	818 (s)	Si-CH ₃ ?
	1007 (m)	"
	1138 (w)	"
	1239 (w)	
	1480 (w)	
	2916 (s)	Si-CH ₃ ?
	2971 (s)	
	3123 (w)	
Uncoated RCC	--	
Tetraethylorthosilicate Coated Material (TEOS)	788 (m)	Si-?
Quartz		
	456 (sb)	Si-O-Si
	833 (m)	"
	1086 (w)	"
Dow Corning Silicon Grease DC-11		
	514 (s)	
	711 (s)	
	806 (w)	Si-O-Si
	1133 (m)	"
	1234 (m)	
	1415 (m)	
	2916 (s)	CH ₃ ? or =CH ₂
	2971 (s)	
	3123 (w)	
w - weak, m - moderate, s - strong, b - broad, v- very		

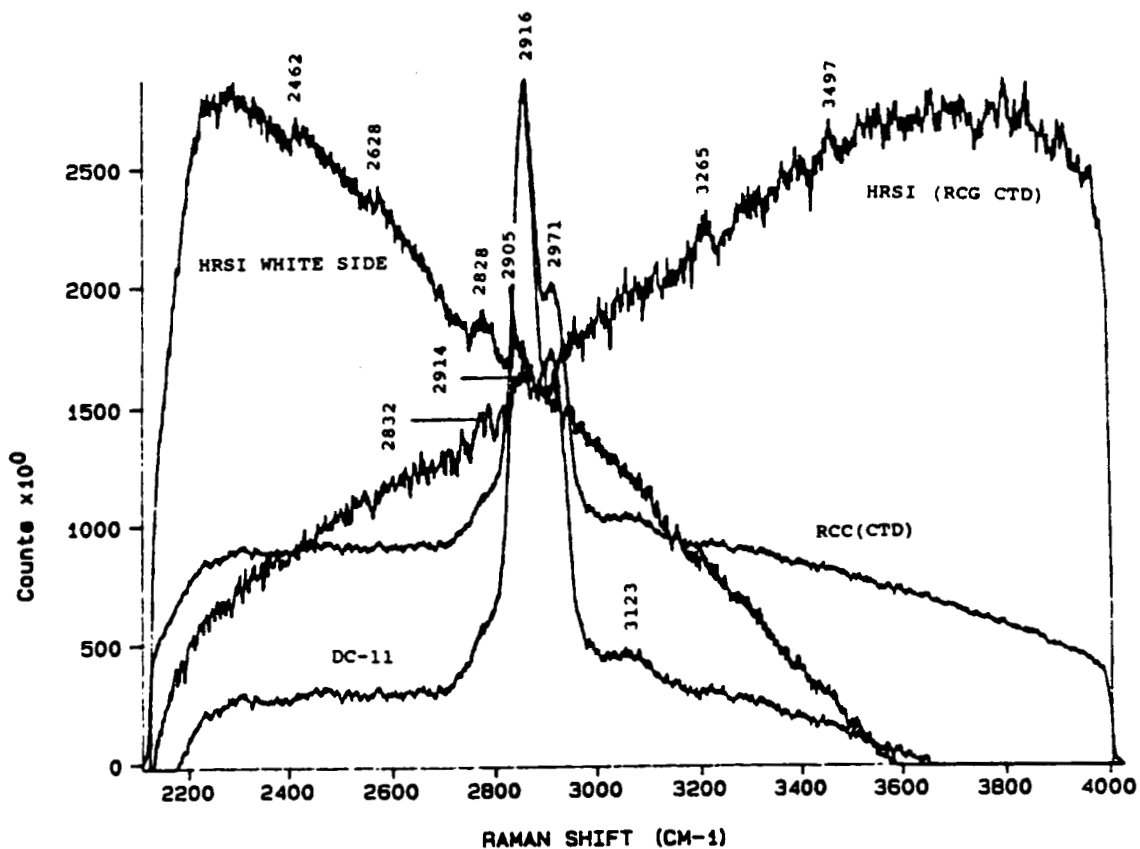


Figure 5. Raman Spectra for Various Materials, 2200 to 4000 cm^{-1} , 514.6 nm Excitation Line.

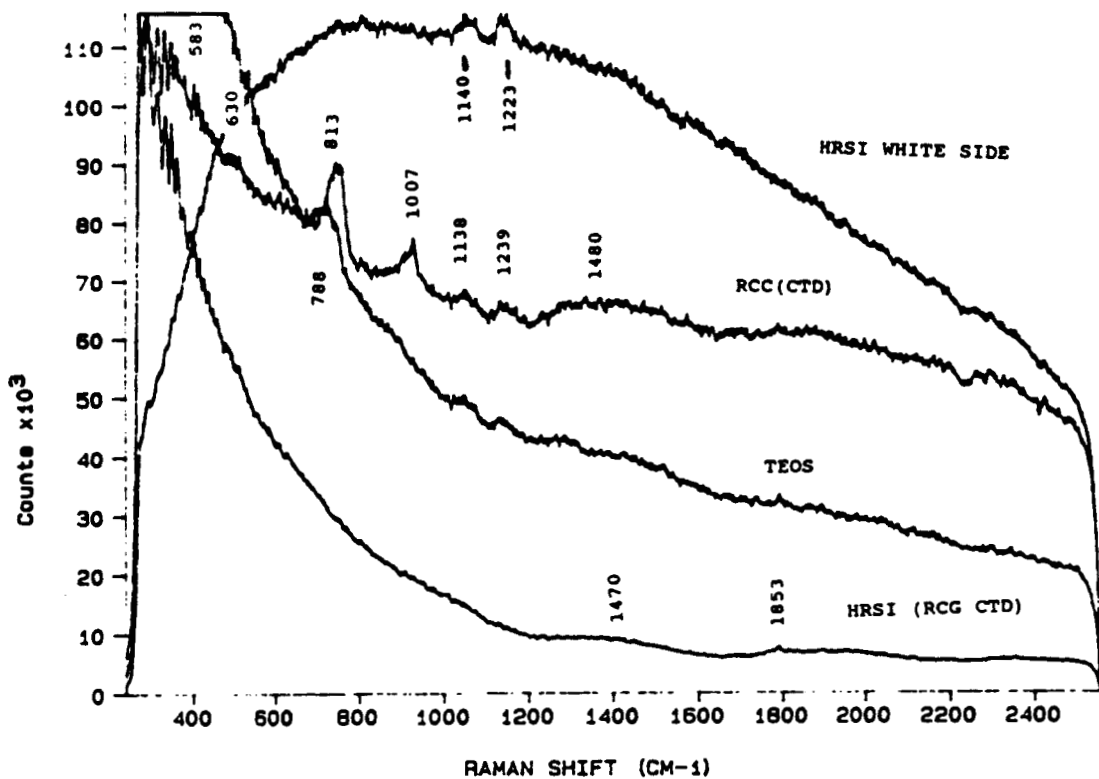


Figure 6. Raman Spectra for HRSI, RCC and TEOS materials, 240 to 2600 cm^{-1} , 514.6 nm Excitation Line.

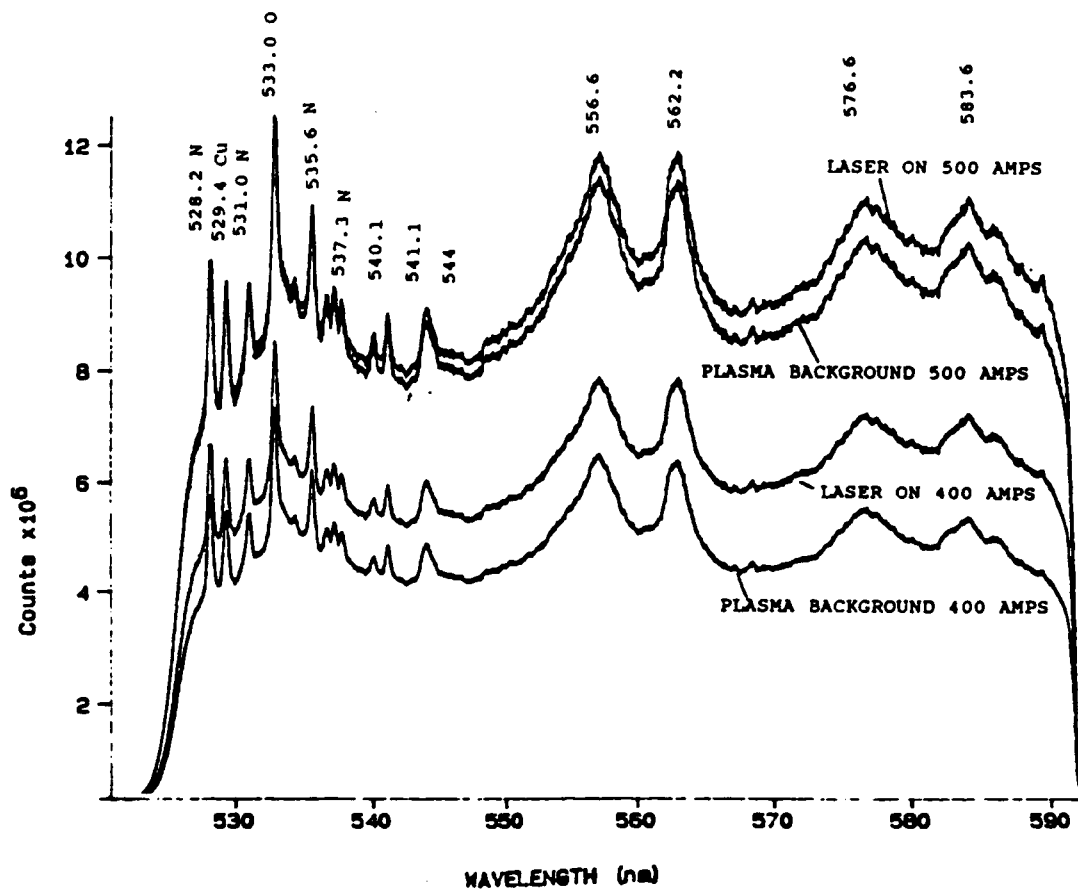


Figure 7. Emission Spectra for a HRSI Hemisphere in an Arc Jet Flow for a Point 1 cm back of the Stagnation Point. 560 nm Centering Wavelength.

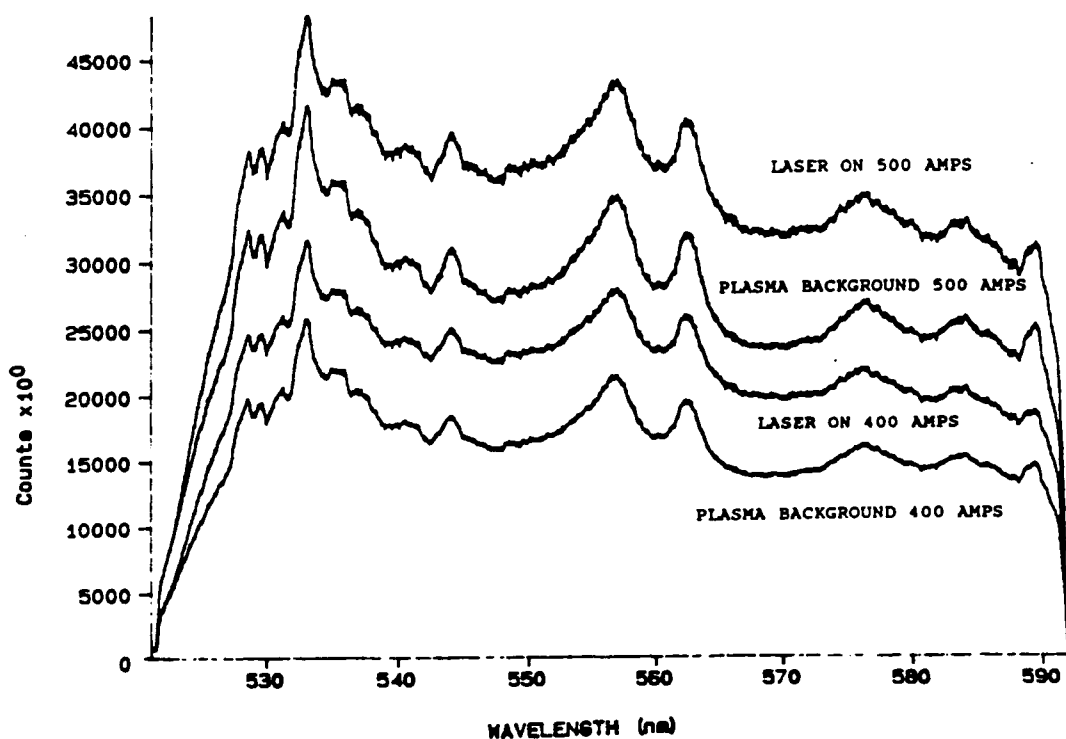


Figure 8. Emission Spectra for a HRSI Hemisphere in an Arc Jet Flow for a Point 3.5 cm back of the Stagnation Point. 560 nm Centering Wavelength.

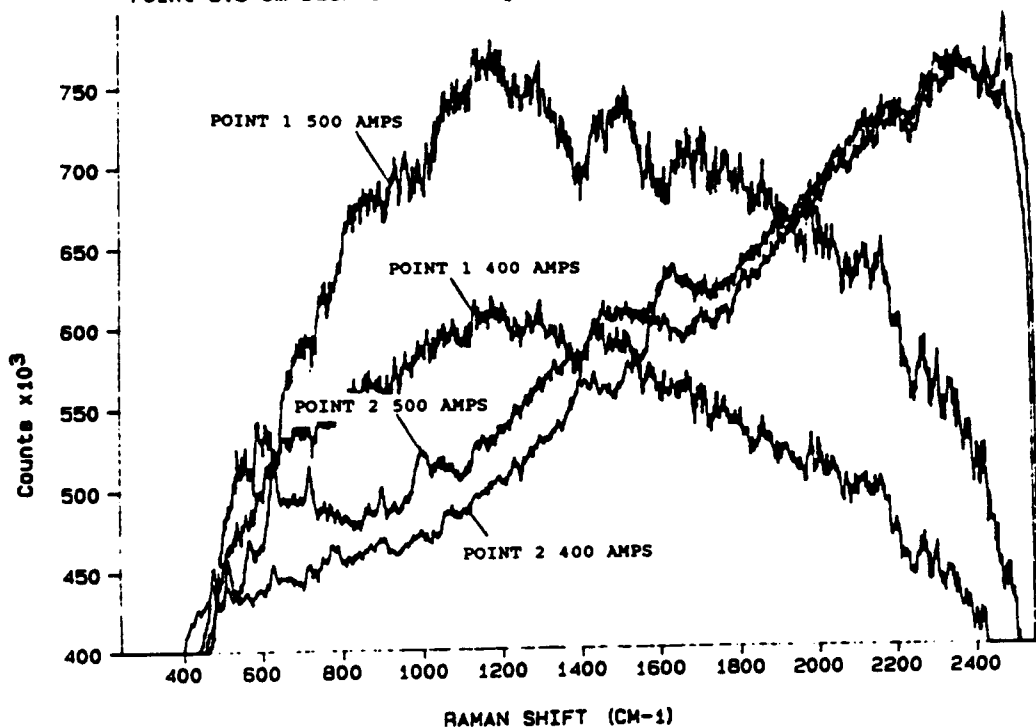


Figure 9. Raman Spectra for a HRSI Hemisphere in an Arc Jet Flow for 1 and 3.2 cm back of the Stagnation Point. 560 nm Centering Wavelength. 514.5 nm Laser Excitation Line.

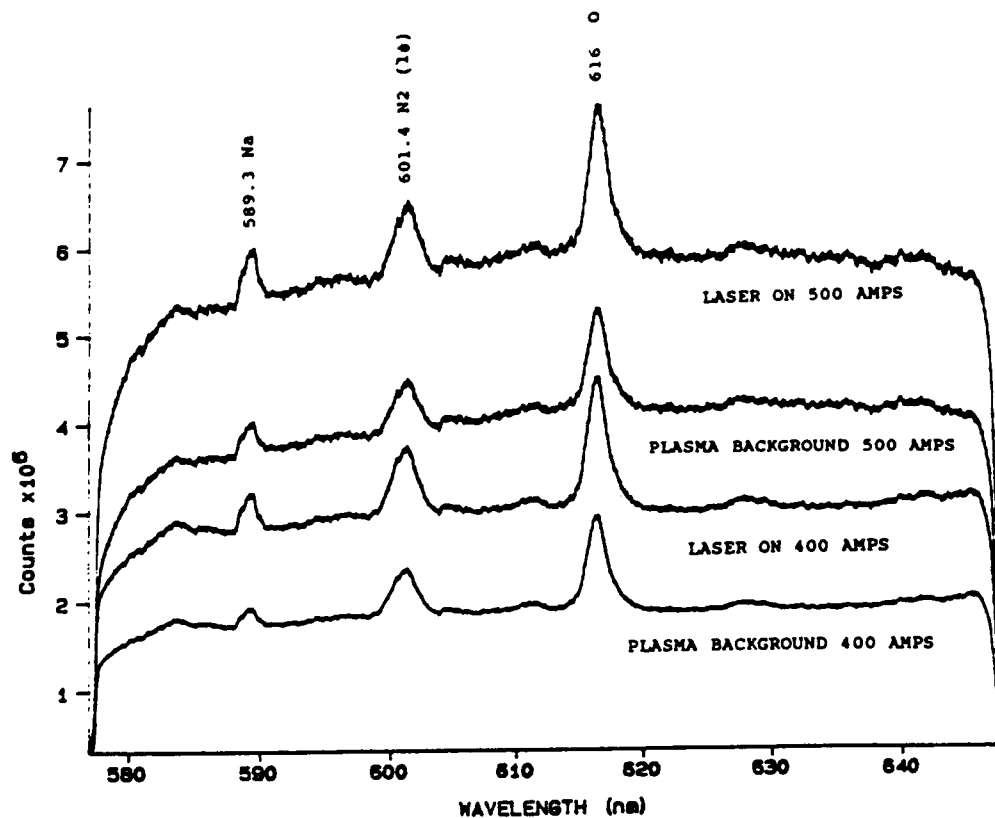


Figure 10. Emission Spectra for a HRSI Hemisphere in an Arc Jet Flow for a Point 3.5 cm back of the Stagnation Point. 616 nm Centering Wavelength.

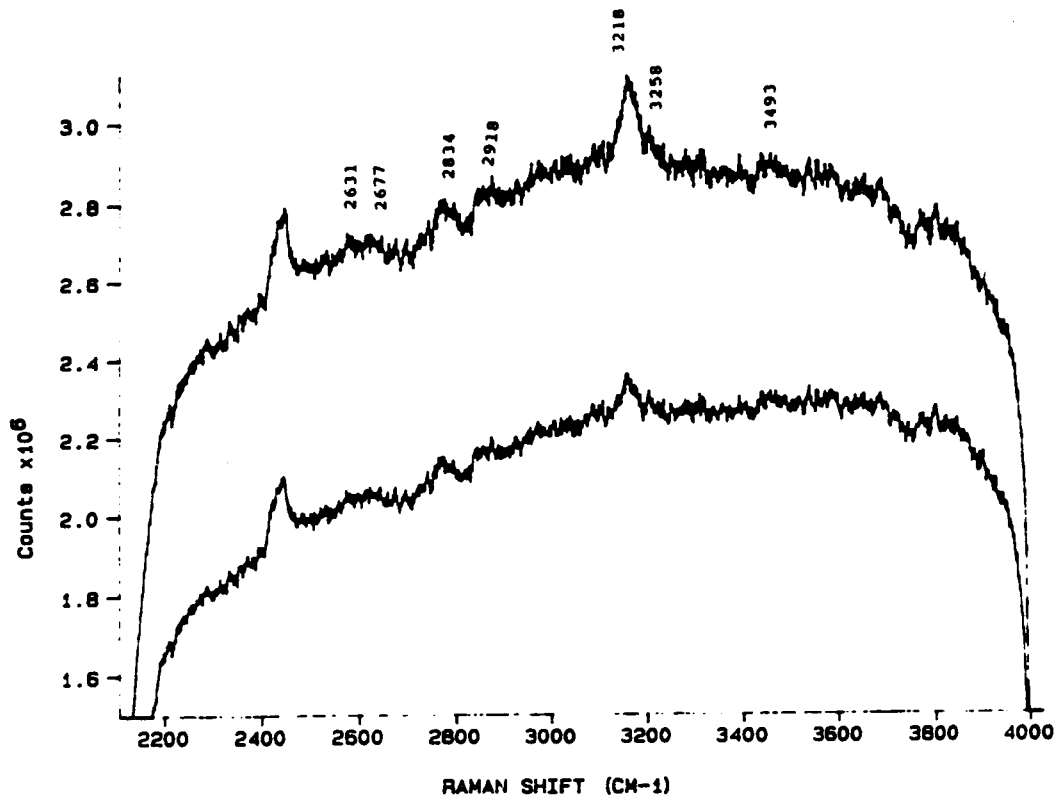


Figure 11. Raman Spectra for a HRSI Hemisphere in an Arc Jet Flow for a Point 3.5 cm back of the Stagnation Point. 616 nm Centering Wavelength. 514.5 nm Laser Excitation Line.

peaks are seen at wavenumbers of 2631, 2677, 2834, 2918, 3258, and 3493 cm^{-1} . Of these peaks, three (2631, 2677, and 3258 cm^{-1}) cannot be related back to the emission spectra and thus may represent Raman shifts. A review of the raw material Raman spectra in Figure 5 shows weak peaks at 2832, 2914, 3265, and 3497 cm^{-1} . So maybe one Raman signal may exist at 3255 to 3265 cm^{-1} . More work is suggested by isolating on this region and investigating it carefully.

Investigation on the HRSI RCG coated wedge model presented a lower temperature condition than that seen with the hemisphere. Results are shown for two current levels of 500 amps and 900 amps in Figure 12. The first noticeable result is lower intensity emission spectra for both plasma background and laser on conditions (see Figure 12). Another observation is how the two spectrums, laser on versus plasma background, differ. In the hemispherical case the laser versus plasma background spectrums were nearly identical with only intensities different. With the wedge model, this is not the case and an explanation should be found.

The difference spectra is shown in Figure 13. Bumps are present but it is difficult to determine if these are Raman shifts or noise. Further investigation is warranted to find out.

CONCLUSIONS

1. Raman spectroscopy is possible with the apparatus available at the JSC Arc Jet.
2. Raman shifts were observed under room temperature and atmospheric pressure conditions for several materials including RCC coated materials and TEOS coated materials. Weak shifts were seen for HRSI materials under the same conditions.
3. Raman shifts could not be easily discerned under arc jet conditions.
4. Laser on conditions influenced emission intensities across the regions scanned (500 to 700 nm). The influence was found to be indirectly related to arc jet temperatures. At high temperatures (1460 K) little change was observed. Where at low temperatures (980 K), major differences were seen between laser on and laser off emission spectrums.

RECOMMENDATIONS

1. Continue Raman spectroscopy investigations with HRSI materials noting the following:
 - a. Confirm that the emission peaks identified are the species so identified.
 - b. Repeat the Raman experiments with the Spex slit closed to 100 microns.
2. Change materials to a RCC coated material which has several good Raman peaks and repeat the Raman spectra experiments under arc jet conditions.
3. Purchase a Spex Model 1460 tunable excitation filter.

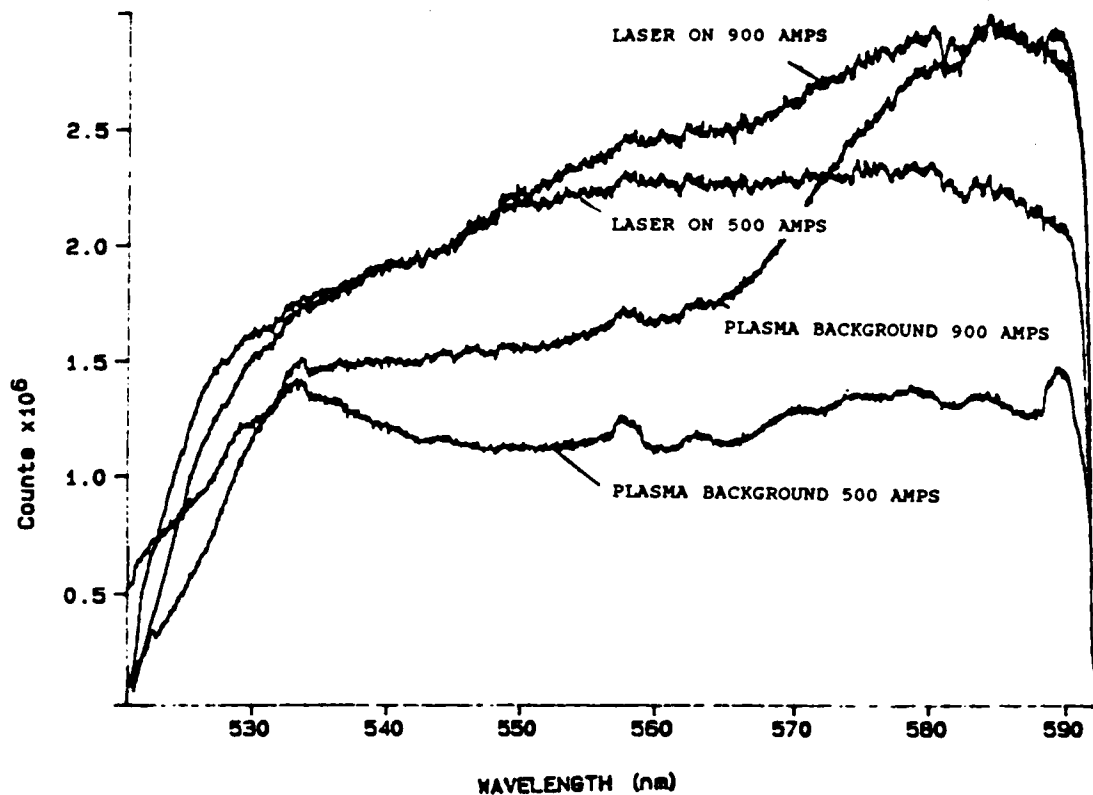


Figure 12. Emission Spectra for a HRSI Wedge in an Arc Jet Flow for a Point 3.5 cm back of the Leading Edge. 560 nm Centering Wavelength.

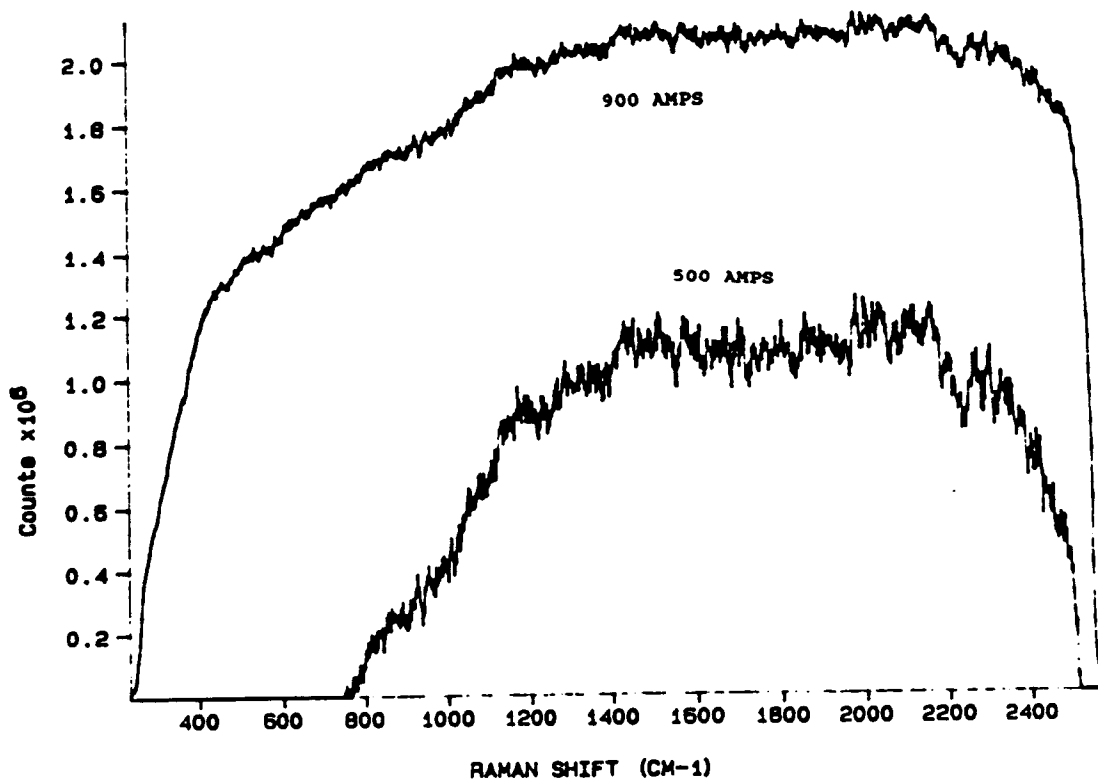


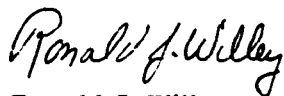
Figure 13. Raman Spectra for a HRSI Wedge in an Arc Jet Flow for a Point 3.5 cm back of the Leading Edge. 560 nm Centering Wavelength. 514.5 nm Laser Excitation Line.

4. Purchase or build a remote control for the Spex filter setting. With a plasma filter, all spectrographic experiments could be conducted inside the control room with fewer arc off requirements.

5. Continue efforts to confirm catalysis/recombination behavior at high temperature conditions. If recombination peaks with temperature do exist, heat shield design criteria may be changed substantially.

ACKNOWLEDGMENTS

I would like to express my gratitude to the many people who assisted me throughout my summer faculty fellowship. Special thanks are extended to Mr. John Grimaud, Dr. Carl Scott, Dr. Fred Wierum, Dr. Harvel Blackwell, Mr. V.S. Murty, Dr. Arepalli, Mr. Ted Heaton, and Mr. William Davis. I would also like to thank the 2nd and 3rd shift arc jet personnel for their assistance in the arc jet experiments. A thanks is extended to the Building 13 Lockheed employees, particularly Mr. Dwayne Castin who performed the infrared spectrum on the Dow Corning silicon grease. It was a pleasure to work with everyone associated with NASA and this project. THANK YOU.



Ronald J. Willey
3 September 1987

REFERENCES

Auerbach, D.R.; Tallant, D.R.; and Higgins, K.L.: Evaluation and Mapping of Heatshield Flight Temperature and Compositions with Laser-Raman Spectroscopic Techniques. AIAA-87-1638, June, 1987.

Bentley, F.F.; Bentley, F.F.; and Smithson, L.D.: Infrared Spectra and Characteristic Frequencies 700-300 cm^{-1} : A Collection of Spectra, Interpretation, and Bibliography. Interscience Publishers, Div. of John Wiley, & Sons, New York, 1968.

Blackwell, H.E.; Wierum, F.A.; and Scott, C.D.: Spectral Determination of Nitrogen Vibrational Temperatures. AIAA-87-1532, June 1987.

Chan, S.S.; and Wachs, I.E.: In Situ Laser Raman Spectroscopy of Nickel Oxide Supported on gamma -Al₂O₃. J. Catal., vol. 103, 1987, pp. 224-227.

Colthup, N.B.; Daly, D.H., and Wilberley, S.E.: Introduction to Infrared and Raman Spectroscopy. Academic Press, New York, 1964.

Eckbreth, A.C.; Bonczyk, P.A.; and Verdick, J.F.: Laser Raman and Fluorescence Techniques for Practical Combustion Diagnostics. Applied Spectroscopy Reviews, vol. 13, no. 1, 1979, pp. 15-167.

Gilson, T.R.; and Hendra, P.J.: Laser Raman Spectroscopy. John Wiley & Sons, Ltd. Bath, G.B., 1970.

Greaves, J.C.; and Linett, J.W.: Recombination of Atoms at Surfaces. Advisory Group for Aeronautical Research and Development Report #332 Paris, 1959.

Greaves, J.C.; and Linett, J.W.: The Recombination of Oxygens Atoms at Surfaces. Trans. of the Faraday Society, vol. 54, Sept., 1958, p. 1323.

Hair, M.L.: Infrared Spectroscopy in Surface Chemistry. Marcel Dekker, Inc., New York, 1967.

Hemley, R.J.; Bell, P.M.; and Mao, H.K.: Laser Techniques in High-Pressure Geophysics. Science, vol. 237, 1987, pp. 605-612.

Herzberg, G.: Atomic Spectra and Atomic Structure. Dover Publications, New York, 1944, p. 10.

JSC Publications Manual: Guidelines for Preparing Scientific and Technical Information for Publication in NASA Formal and Informal Documents. JSCM 2220, Mar. 1984.

Jumper, E.J.; Ultee, C.J.; Dorko, E.A.: A Model for Fluorine Atom Recombination on a Nickel Surface. J. Phys. Chem., vol. 84, 1980, pp. 41-50.

Kolodziej, P.; Stewart, D.A.: Nitrogen Recombination on High Temperature Reusable Surface Insulation and the Analysis of its Effect on Surface Catalysis. AIAA-87-1637, June, 1987.

Morrow, B.A.: Raman Spectroscopic Studies of Surface Species. in Vibrational Spectroscopies for Adsorbed Species. ACS Sym. Ser. 137 1980.

Nordine, P.C.; Fujimoto, G.T.; and Greene, F.T.: The Study of Excited Oxygen Molecule Gas Species Production and Quenching on Thermal Protection System Materials. Final Report NASA Contract No. NAS9-17261, June 24, 1987.

Pearse, R.W.B.; and Gaydon, A.G.: The Identification of Molecular Spectra. Chapman & Hall, London, 1965.

Rochelle, W.C.; Battley, H.H.; Grimaud, J.E.; Tillian, D.J.; Murray, L.P.; Lueke, W.J.; and Heaton, T.M.: Orbiter TPS Development and Certification Testing At the NASA/JSC 10 MW Atmospheric Reentry Materials and Structures Evaluation Facility. AIAA-83-0147, Jan 1983.

Scott, C.D.: Effect of Nonequilibrium and Wall Catalysis on Shuttle Heat Transfer. Journal of Spacecraft and Rockets, vol. 22, no. 5, Sept-Oct, 1985, pp. 489-499.

Seward, W.A.: A Model for Oxygen Atom Recombination on a Silicon Dioxide Surface. AFIT/DS/AA/85-1, Ph.D. Dissertation, Air Force Institute of Technology, 1985.

Stewart, D.A.; and Leiser, D.B.: Catalytic Surface Effect on Ceramic Coatings for an Aeroassisted Orbital Transfer Vehicle. Ceramic Engineering and Science Proceedings, vol. 5, March, 1984, pp. 491-505.

The Encyclopedia Britannica: Encyclopedia Britannica, Inc. Chicago, 15th Ed., 1985, pp. 9:917, 13:554-581.

Wachs, I.E.; Hardcastle, F.D.; and Chan, S.S.: Raman Spectroscopy of Supported Metal Oxide Catalysts. Spectroscopy, vol. 1, no. 8, 1986.

Wierum, F.A.: 1984 ASEE-NASA Summer Faculty Fellowship Final Report. NASA-JSC 1984.

Willey, R.J.: The Identification of Excited Species in Arc Jet flow. NASA CR 171990, August 15, 1987.

Wise, H.; Wood, B.J.: Reactive Collisions Between Gas and Surface Atoms. Adv. in Atomic & Molecular Physics, vol. 3, 1967, pp. 291-353.